J Low Temp Phys (2018) 191:408–425
https://doi.org/10.1007/s10909-018-1882-7

Stability of the Superconducting d-Wave Pairing Toward the Intersite Coulomb Repulsion in CuO_2 Plane

V. V. Val'kov[1] · D. M. Dzebisashvili[1,2] · M. M. Korovushkin[1] · A. F. Barabanov[3]

Received: 29 September 2017 / Accepted: 20 February 2018 / Published online: 1 March 2018

Abstract Taking into account the real crystalline structure of the CuO_2 plane and the strong spin-fermion coupling, we study the influence of the intersite Coulomb repulsion between holes on the Cooper instability of the spin-polaron quasiparticles in cuprate superconductors. The analysis shows that only the superconducting d-wave pairing is implemented in the whole region of doping, whereas the solutions of the self-consistent equations for the s-wave pairing are absent. It is shown that intersite Coulomb interaction V_1 between the holes located at the nearest oxygen ions does not affect the d-wave pairing, because its Fourier transform V_q vanishes in the kernel of the corresponding integral equation. The intersite Coulomb interaction V_2 of quasiparticles located at the next-nearest oxygen ions does not vanish in the integral equations, however, but it is also shown that the d-wave pairing is robust toward this interaction for physically reasonable values of V_2.

Keywords Cuprate superconductors · Unconventional superconductivity · Spin-charge coupling · Spin polarons · Intersite Coulomb interaction

1 Introduction

An analysis of the normal phase of cuprate superconductors has proved the Mott–Hubbard-type insulator ground state [1–4] of these materials. When this conclusion

✉ M. M. Korovushkin
kmax@iph.krasn.ru

1 Kirensky Institute of Physics, Federal Research Center KSC SB RAS, Krasnoyarsk, Russia 660036

2 Siberian State University of Science and Technology, Krasnoyarsk, Russia 660037

3 Vereshchagin Institute for High Pressure Physics, Troitsk, Moscow, Russia 108840

was reached, it became clear that one should study cuprates at low doping on the basis of the Hubbard model [3] in the regime of strong electron correlations (SEC). In Ref. [1], the subsystem of copper spin momenta was considered within the resonating valence bond theory and the charge excitations arising from the doping were interpreted as a fermionic subsystem exhibiting the Cooper instability. Such a mechanism of superconductivity was of electronic nature and resulted in high values of the critical temperatures T_c.

Since a number of experimental data indicated that the main dynamics of Fermi excitations takes place in the CuO_2 planes [5,6], the 2D Hubbard model on a simple square lattice was widely used to describe unconventional superconductivity in cuprates [7–16]. An important issue concerning the role of the long-range part of Coulomb interaction in the problem of unconventional superconductivity was raised in Ref. [17]. The authors noted that the majority of previous investigations was limited to the short-range Coulomb interaction U having in mind the computational difficulties connected with taking into account the Fourier transform of the intersite Coulomb repulsion $V_{\mathbf{q}}$. The rising interest in the role of the intersite Coulomb interaction in the structure of the phase diagram of high-temperature superconductors has made the extended Hubbard model (the Shubin–Vonsovsky model [18]) popular [19–22]. This model takes into account not only one-site Hubbard repulsion, but the interaction of electrons at different sites of the crystalline lattice within several coordination spheres. In Refs. [20–22], a phase diagram presenting the result of competition of superconducting phases with different types of order parameter symmetry was calculated in the Born weak-coupling approximation.

However, along with a number of important results on the normal and superconducting properties of cuprates obtained in the framework of the Hubbard model and extended Hubbard model, it appeared that one had not taken into account specific features of the real structure of materials. A minimal realistic microscopic model for cuprates was proposed by Emery [23]. The three-band Emery model takes into account the real structure of the CuO_2 plane which is characterized by the spatial separation of the subsystem of oxygen holes and the subsystem of the localized copper spins. Besides, this model considers the $d_{x^2-y^2}$-orbitals of copper ions and p_x- and p_y-orbitals of oxygen ions (Fig. 1). An account for the on-site Coulomb correlations allowed one to pass to the regime of SEC and describe the Mott–Hubbard ground state in the case of one hole per unit cell. In Ref. [24], it was shown that doping of one extra-hole in the CuO_2 plane leads to the formation of a spin-singlet state of a copper hole and a hole moving along the binding oxygen orbital (the Zhang–Rice singlet). In this context, investigations concerning the possibility of obtaining the effective one-band Hubbard-like models for cuprate superconductors have been carried out [25–28]. As a result, a number of studies in this direction were performed in the framework of the $t-J$ and $t-J^*$ models on a simple square lattice. Within such an approach, the same fermions formed both the charge and the spin subsystems, and the superconducting d-wave pairing was initiated by the exchange and the spin-fluctuation mechanisms [29–33].

Thus, on the fundamental level, it would seem that the nature of an effective attraction between the Hubbard fermions was revealed. However, there remained a problem related to the intersite Coulomb repulsion of oxygen holes. The point

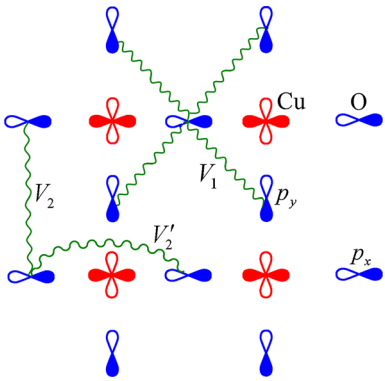

Fig. 1 Structure of CuO_2 plane. Here V_1 denotes the Coulomb interaction between holes located at the nearest-neighbor oxygen sites, V_2 and V_2' are the interactions between holes at the next-nearest-neighbor oxygen sites (Color figure online)

is that the Cooper pairing of fermions caused by the kinematic [9], exchange and spin-fluctuation mechanisms considered in the Hubbard [34,35], $t-J$ [30–33], or $t-J^*$ [36,37] models is suppressed by the intersite Coulomb repulsion V_1 of charge carriers located at the neighboring sites. This effect is most pronounced in the superconducting d-wave channel [38,39] and, as a result, the Cooper instability disappears completely at V_1 ranging from 1 to 2 eV. Hence, in order to compensate the strong repulsive interaction, it was necessary to take into consideration additional contributions connected with the electron-phonon [40], spin-fluctuation [41] and charge-fluctuation interactions [38,39,42]. In Refs. [38,39,42], the value $V_1 = 0.2$ eV for the intersite Coulomb interaction was used. Such a value, which was found for holes located at the nearest-neighbor unit cells in the framework of the cluster perturbation theory [27,43], is significantly less than the value of spin-fluctuation pairing $g_{sf} = 1.5$ eV, therefore the superconducting d-wave pairing was preserved. Indeed, the Wannier transform of the Hamiltonian reduces the initial value of the intersite interaction to $V_1 \leq 0.3\,\text{eV}$, but at the same time generates the Coulomb interactions between holes located at the distant sites [44]. Such distant interactions are always ignored within the cluster calculations, despite the fact they result in significant renormalization of the Fermi excitation spectrum [45]. Though, the cluster perturbation theory takes into account the strong intra-atomic interactions rigorously, the correct description of the Coulomb interaction between fermions located at the nearest-neighbor and especially distant unit cells remains problematical (see, for example, [46]). For the superconducting s-wave pairing caused by the kinematic interaction [9], Cooper pairing was implemented even at high values of V_1. It should be noted that an argument connected with the screening of the Coulomb interaction was sometimes used. However, in this case, it is not very convincing, as it relates to the repulsion between holes at the nearest distances [34] and the case of low densities [47].

The problem of neutralization the Coulomb repulsion between oxygen holes demanded a revision of existing theories of the Cooper instability in cuprates. In this regard, it is pertinent to note that a similar problem existed in the past in the theory of classical superconductors (see, for example, review [48]). The problem was solved by the authors of Refs. [49,50], who showed that electron-phonon interaction in some

region of the momentum space initiates an effective attraction between fermions. This effective attraction can compensate the bare Coulomb repulsion.

In our previous paper [51], it has been shown that the solution for the problem of the superconducting d-wave pairing stability toward the intersite Coulomb interaction in cuprates is connected with the rejection of the Hubbard model as well as its effective low-energy variants and a return to the model describing the real structure of the CuO_2 plane. As such a model, the spin-fermion model (SFM) [46,52–57] was used which was obtained in the early stages of the development of cuprate superconductors theory. The SFM follows directly from the Emery model [23] and takes into account by perturbation theory the effects of covalent mixing between copper and oxygen orbitals. It is essential that the SFM takes into account the two-orbital character of the oxygen subsystem and the spatial separation between the oxygen and copper subsystems. In Ref. [51] it was shown that an account of the above-mentioned features of the SFM leads to the stability of the superconducting $d_{x^2-y^2}$-wave pairing with respect to the intersite Coulomb repulsion.

However, in Ref. [51] the mentioned stability was proved only for the case of intersite Coulomb repulsion of holes located at the nearest-neighbor oxygen ions V_1, while the role of repulsion between holes located at the more distant oxygen ions remains unclear (the influence of V_2 on the superconducting d-wave pairing has been also mentioned in Ref. [42]). Additionally, the possibility of the superconducting s-wave pairing in the SFM remains unclear. Note that in Refs. [38,39,42] it was claimed that for the Hubbard model in the limit of SEC, where the projected electron operators are used, the s-wave pairing is prohibited since it violates the fundamental rigorous restriction of no double occupancy of a quantum state at any lattice site. However, such a restriction is absent in the SFM, since the carriers are the holes moving over oxygen ions.

In this paper, we study the influence of the Coulomb interaction between holes at the next-nearest-neighbor oxygen ions of the CuO_2-plane on the superconducting $d_{x^2-y^2}$-wave and s-wave pairings.

2 Spin-Fermion Model

It is known that the main features of the electronic structure of the CuO_2 planes can be described by the Emery model [23,47]. In accordance with experimental data, without doping (one hole per unit cell), the ground state of the system is the Mott–Hubbard insulator [2]. In the Emery model, the regime of SEC

$$\Delta_{\mathrm{pd}}, (U_d - \Delta_{\mathrm{pd}}) \gg t_{\mathrm{pd}} > 0 \tag{1}$$

corresponds to such a ground state. These inequalities, on the one hand, require rigorous accounting of the Coulomb correlations and, on the second hand, allow one to reduce the Emery Hamiltonian and obtain the SFM [46,52–57] describing the subsystem of oxygen holes interacting with the localized copper spins. The Hamiltonian is given by

$$\hat{H}_{\mathrm{sp}-f} = \hat{H}_h + \hat{U}_p + \hat{V}_{\mathrm{pp}} + \hat{J} + \hat{I}, \tag{2}$$

where

$$\begin{aligned}
\hat{H}_h &= \sum_{k\alpha}\Big(\xi_{k_x} a^\dagger_{k\alpha} a_{k\alpha} + \xi_{k_y} b^\dagger_{k\alpha} b_{k\alpha} + t_k (a^\dagger_{k\alpha} b_{k\alpha} + b^\dagger_{k\alpha} a_{k\alpha})\Big),\\
\hat{U}_p &= \frac{U_p}{N} \sum_{1,2,3,4} \Big[a^\dagger_{1\uparrow} a^\dagger_{2\downarrow} a_{3\downarrow} a_{4\uparrow} + (a \to b)\Big]\ \delta_{1+2-3-4},\\
\hat{V}_{\mathrm{pp}} &= \frac{4V_1}{N} \sum_{\substack{1,2,3,4\\ \alpha\beta}} \phi_{3-2}\ a^\dagger_{1\alpha} b^\dagger_{2\beta} b_{3\beta} a_{4\alpha}\ \delta_{1+2-3-4}\\
&\quad + \frac{V_2}{N} \sum_{\substack{1,2,3,4\\ \alpha\beta}} \theta^{xy}_{2-3}\ a^\dagger_{1\alpha} a^\dagger_{2\beta} a_{3\beta} a_{4\alpha}\ \delta_{1+2-3-4}\\
&\quad + \frac{V_2}{N} \sum_{\substack{1,2,3,4\\ \alpha\beta}} \theta^{yx}_{2-3}\ b^\dagger_{1\alpha} b^\dagger_{2\beta} b_{3\beta} b_{4\alpha}\ \delta_{1+2-3-4},\\
\hat{J} &= \frac{J}{N} \sum_{fkq\alpha\beta} e^{if(q-k)} u^\dagger_{k\alpha} (\mathbf{S}_f \boldsymbol{\sigma}_{\alpha\beta}) u_{q\beta},\\
\hat{I} &= \frac{I}{2} \sum_{f\delta} \mathbf{S}_f \mathbf{S}_{f+2\delta}.
\end{aligned}$$

Here

$$\begin{aligned}
&\xi_{k_{x(y)}} = \varepsilon_p + 2V_{\mathrm{pd}} + \tau(1-\cos k_{x(y)}) - \mu, \qquad t_k = (2\tau - 4t) s_{k,x} s_{k,y},\\
&s_{k,x} = \sin\frac{k_x}{2}, \qquad \theta^{xy(yx)}_k = \frac{V_2'}{V_2} e^{ik_{x(y)}} + e^{-ik_{y(x)}}, \quad u_{k\beta} = s_{k,x} a_{k\beta} + s_{k,x} b_{k\beta},\\
&\tau = \frac{t^2_{\mathrm{pd}}}{\Delta_{\mathrm{pd}}}\left(1 - \frac{\Delta_{\mathrm{pd}}}{U_d - \Delta_{\mathrm{pd}} - 2V_{\mathrm{pd}}}\right), \quad J = \frac{4t^2_{\mathrm{pd}}}{\Delta_{\mathrm{pd}}}\left(1 + \frac{\Delta_{\mathrm{pd}}}{U_d - \Delta_{\mathrm{pd}} - 2V_{\mathrm{pd}}}\right).
\end{aligned} \tag{3}$$

The Hamiltonian $\hat{H}_h$ describes the oxygen holes in the momentum representation. Here $a^\dagger_{k\alpha}(a_{k\alpha})$ are the hole creation (annihilation) operators in the oxygen subsystem with the p_x-orbitals (Fig. 1), $\alpha = \pm 1/2$ is the spin projection. Similarly, $b^\dagger_{k\alpha}(b_{k\alpha})$ are operators in the oxygen subsystem with the p_y-orbitals. The bare one-site energy of oxygen holes is ε_p, μ is the chemical potential, and t is the hopping integral. The operator $\hat{J}$ describes the exchange interaction between the oxygen subsystem and the subsystem of the spins localized at copper ions. Here, $\mathbf{S}_f$ is the operator of a spin localized at the site with index f and $\boldsymbol{\sigma} = (\sigma^x, \sigma^y, \sigma^z)$ is the vector of the Pauli matrices. The operator $\hat{I}$ describes the superexchange interaction between the neighboring copper spins arising in the fourth order of the perturbation theory. The

intersite Coulomb interaction between holes (Fig. 1) is described by the operator $\hat{V}$. In the Hamiltonian, $\hat{n}_{f+x(y)/2} = \sum_\sigma \hat{n}_{f+x(y)/2,\sigma}$ are the operators of the number of holes at the oxygen site $f + x(y)/2$. Here, $x = (1, 0)$ and $y = (0, 1)$ are the lattice basis vectors in the units of the lattice parameter.

When writing the Hamiltonian (2), we take into account that the hopping integrals in the first and the second terms can have different signs for different hopping directions owing to the different phases of the wave functions. For the sake of compactness, we denote momenta over which the summation is performed by numbers 1,…,4. The Dirac delta-function $\delta_{1+2-3-4}$ takes into account the momentum conservation law.

Below, we use the commonly accepted set of parameters for the Emery model: $t_{\rm pd} = 1.3\,{\rm eV}$, $\Delta_{\rm pd} = 3.6\,{\rm eV}$, $U_d = 10.5\,{\rm eV}$, $V_{\rm pd} = 1.2\,{\rm eV}$ [58,59]. For the hopping integral of the holes, we use the value $t = 0.12$ eV [60] and suppose that the superexchange parameter $I = 0.136\,{\rm eV}$ (1570 K) in accordance with experimental data on cuprate superconductors [59]. For the parameters of the intersite Coulomb interactions, we suppose that V_1 is ranging from 1 to 2 eV [61] and V_2 and V_2' are ranging from 0.5 to 1 eV.

3 Equations for Green's Functions

It is important that the exchange energy between the localized and itinerant spins within the SFM is large, namely, $J = 3.38\,{\rm eV} \gg \tau \approx 0.47\,{\rm eV}$. Therefore, to describe the dynamics of oxygen holes it is necessary to take into consideration the exchange interaction rigorously. This problem can be solved in the framework of the Zwanzig–Mori projection technique [62,63]. The calculation method of the energy structure of the spin-polaron quasiparticles based on this technique within the SFM was described in detail in Refs. [60,64–66]. In accordance with this method, it is essential to introduce, besides $a_{k\alpha}$ and $b_{k\alpha}$, another operator

$$L_{k\alpha} = \frac{1}{N} \sum_{fq\beta} e^{if(q-k)} (\mathbf{S}_f \boldsymbol{\sigma}_{\alpha\beta}) u_{q\beta}, \tag{4}$$

which describes the strong spin-charge coupling. To consider the Cooper instability, it is required to supply the basis set $\{a_{k\alpha},\ b_{k\alpha},\ L_{k\alpha}\}$ by the operators

$$a^\dagger_{-k\bar{\alpha}}, \quad b^\dagger_{-k\bar{\alpha}}, \quad L^\dagger_{-k\bar{\alpha}}, \tag{5}$$

where $\bar{\alpha} = -\alpha$. Supplementation of these operators allows one to study not only the normal, but the anomalous thermodynamic means within an unified approach.

In the framework of the projection technique [62,63], the system of equations for Green's functions can be represented in the matrix form

$$\omega\, \hat{G}(k, \omega) = \hat{K}(k) + \hat{D}(k) \hat{K}^{-1}(k)\, \hat{G}(k, \omega), \tag{6}$$

where the retarded Green's function matrix is determined by the elements $G_{ij}(k, \omega) = \langle\langle A_{ik} | A^\dagger_{jk} \rangle\rangle_\omega$, and the elements of energetic $\hat{D}(k)$ and normalization $\hat{K}(k)$ matrices are given by the expressions

$$D_{ij}(k) = \left\langle\{[A_{ik}, \hat{H}_{\mathrm{sp}-f}], A^{\dagger}_{jk}\}\right\rangle, \qquad K_{ij}(k) = \left\langle\{A_{ik}, A^{\dagger}_{jk}\}\right\rangle. \tag{7}$$

The operators A_{ik} on the right side of the expressions (7) run over the set of six basis operators

$$\{a_{k\uparrow}, b_{k\uparrow}, L_{k\uparrow}, a^{\dagger}_{-k\downarrow}, b^{\dagger}_{-k\downarrow}, L^{\dagger}_{-k\downarrow}\}, \tag{8}$$

and the brackets $\langle\ldots\rangle$ denote the thermodynamic mean.

After the calculation of the elements (7) and the substitution to the matrix equation (6), the set of equations for the normal G_{ij} and anomalous F_{ij} Green's functions can be represented in the form ($j = 1, 2, 3$)

$$\begin{aligned}
(\omega - \xi_x)G_{1j} &= \delta_{1j} + t_k G_{2j} + J_x G_{3j} + \Delta_{1k}F_{1j} + \Delta_{2k}F_{2j},\\
(\omega - \xi_y)G_{2j} &= \delta_{2j} + t_k G_{1j} + J_y G_{3j} + \Delta_{3k}F_{1j} + \Delta_{4k}F_{2j},\\
(\omega - \xi_L)G_{3j} &= \delta_{3j}K_k + (J_x G_{1j} + J_y G_{2j})K_k + \frac{\Delta_{5k}}{K_k}F_{3j},\\
(\omega + \xi_x)F_{1j} &= \Delta^{*}_{1k}G_{1j} + \Delta^{*}_{3k}G_{2j} - t_k F_{2j} + J_x F_{3j},\\
(\omega + \xi_y)F_{2j} &= \Delta^{*}_{2k}G_{1j} + \Delta^{*}_{4k}G_{2j} - t_k F_{1j} + J_y F_{3j},\\
(\omega + \xi_L)F_{3j} &= \frac{\Delta^{*}_{5k}}{K_k}G_{3j} + (J_x F_{1j} + J_y F_{2j})K_k.
\end{aligned} \tag{9}$$

Here, $G_{11} = \langle\langle a_{k\uparrow}|a^{\dagger}_{k\uparrow}\rangle\rangle$, $G_{21} = \langle\langle b_{k\uparrow}|a^{\dagger}_{k\uparrow}\rangle\rangle$, and $G_{31} = \langle\langle L_{k\uparrow}|a^{\dagger}_{k\uparrow}\rangle\rangle$. The functions G_{i2} and G_{i3} are determined in a similar way with the only difference that $a^{\dagger}_{k\uparrow}$ is replaced by $b^{\dagger}_{k\uparrow}$ and $L^{\dagger}_{k\uparrow}$, respectively. The anomalous Green's functions are defined as $F_{11} = \langle\langle a^{\dagger}_{-k\downarrow}|a^{\dagger}_{k\uparrow}\rangle\rangle$, $F_{21} = \langle\langle b^{\dagger}_{-k\downarrow}|a^{\dagger}_{k\uparrow}\rangle\rangle$, $F_{31} = \langle\langle L^{\dagger}_{-k\downarrow}|a^{\dagger}_{k\uparrow}\rangle\rangle$. For F_{i2} and F_{i3}, the same type of notation regarding the second index is used. The functions involved in the system (9) are given by the expressions

$$\begin{aligned}
&\xi_{x(y)} = \xi_0(k_{x(y)}), \qquad J_{x(y)} = J s_{k,x(y)}, \qquad K_k = \left\langle\{L_{k\uparrow}, L^{\dagger}_{k\uparrow}\}\right\rangle = \frac{3}{4} - C_1\gamma_{1k},\\
&\xi_L(k) = \varepsilon_p - \mu - 2t + 5\tau/2 - J + [(\tau - 2t)(-C_1\gamma_{1k} + C_2\gamma_{2k})\\
&\qquad + \frac{\tau}{2}(-C_1\gamma_{1k} + C_3\gamma_{3k}) + JC_1(1 + 4\gamma_{1k})/4 - IC_1(\gamma_{1k} + 4)]K_k^{-1}.
\end{aligned} \tag{10}$$

Here, γ_{jk} are the square lattice invariants: $\gamma_{1k} = (\cos k_x + \cos k_y)/2$, $\gamma_{2k} = \cos k_x \cos k_y$, $\gamma_{3k} = (\cos 2k_x + \cos 2k_y)/2$.

The introduced superconducting-order parameters $\Delta_{j,k}$

$$\begin{aligned}
\Delta_{1k} &= \left\langle\{[a_{k\uparrow}, \hat{H}_{\mathrm{sp}-f}], a_{-k\downarrow}\}\right\rangle, \quad \Delta_{4k} = \left\langle\{[b_{k\uparrow}, \hat{H}_{\mathrm{sp}-f}], b_{-k\downarrow}\}\right\rangle,\\
\Delta_{2k} &= \left\langle\{[a_{k\uparrow}, \hat{H}_{\mathrm{sp}-f}], b_{-k\downarrow}\}\right\rangle, \quad \Delta_{5k} = \left\langle\{[L_{k\uparrow}, \hat{H}_{\mathrm{sp}-f}], L_{-k\downarrow}\}\right\rangle,\\
\Delta_{3k} &= \left\langle\{[b_{k\uparrow}, \hat{H}_{\mathrm{sp}-f}], a_{-k\downarrow}\}\right\rangle,
\end{aligned} \tag{11}$$

are related to the anomalous averages as follows

$$
\begin{aligned}
\Delta_{1k} &= -\frac{2}{N}\sum_q\Big(\frac{U_p}{2}+V_2\cos(k_y-q_y)+V_2'\cos(k_x-q_x)\Big)\left\langle a_{q\uparrow}a_{-q\downarrow}\right\rangle,\\
\Delta_{2k} &= -\frac{4V_1}{N}\sum_q\phi_{k-q}\left\langle a_{q\uparrow}b_{-q\downarrow}\right\rangle,\\
\Delta_{3k} &= -\frac{4V_1}{N}\sum_q\phi_{k-q}\left\langle b_{q\uparrow}a_{-q\downarrow}\right\rangle,\\
\Delta_{4k} &= -\frac{2}{N}\sum_q\Big(\frac{U_p}{2}+V_2\cos(k_x-q_x)+V_2'\cos(k_y-q_y)\Big)\left\langle b_{q\uparrow}b_{-q\downarrow}\right\rangle,\\
\Delta_{5k} &= \frac{1}{N}\sum_q\Big\{I_{k-q}\big(\left\langle L_{q\uparrow}L_{-q\downarrow}\right\rangle-C_1\left\langle u_{q\uparrow}u_{-q\downarrow}\right\rangle\big)+8IC_1\left\langle u_{q\uparrow}u_{-q\downarrow}\right\rangle\Big\}\\
&\quad+\frac{J}{N}\sum_q\Big\{-2\gamma_{1q}\left\langle L_{q\uparrow}L_{-q\downarrow}\right\rangle+\big(3/2-4C_1\gamma_{1k}\big)\left\langle u_{q\uparrow}u_{-q\downarrow}\right\rangle\Big\}\\
&\quad+\frac{2}{N}\sum_q\big(\xi(q_x)s_{q,x}+t_qs_{q,y}\big)\left\langle a_{q\uparrow}L_{-q\downarrow}\right\rangle\\
&\quad+\frac{2}{N}\sum_q\big(\xi(q_y)s_{q,y}+t_qs_{q,x}\big)\left\langle b_{q\uparrow}L_{-q\downarrow}\right\rangle\\
&\quad-\frac{U_p}{N}\sum_q\Big\{\Big(3/8-\frac{C_1}{2}\cos k_x\Big)\left\langle a_{q\uparrow}a_{-q\downarrow}\right\rangle+\Big(3/8-\frac{C_1}{2}\cos k_y\Big)\left\langle b_{q\uparrow}b_{-q\downarrow}\right\rangle\Big\}\\
&\quad-\frac{V_1}{N}\sum_q\Big\{(3/4-2C_1\gamma_{1k}+C_2\gamma_{2k})\psi_q+C_2\sin k_x\sin k_y\phi_q\Big\}\big(\left\langle a_{q\uparrow}b_{-q\downarrow}\right\rangle\\
&\quad+\left\langle b_{q\uparrow}a_{-q\downarrow}\right\rangle\big)-\frac{1}{N}\sum_q\Big\{V_2(C_1\cos k_y-C_2\gamma_{2k})\cos q_y\\
&\quad+V_2'\Big(-\frac{3}{8}+C_1\cos k_x-\frac{C_3}{2}\cos 2k_x\Big)\cos q_x\Big\}\left\langle a_{q\uparrow}a_{-q\downarrow}\right\rangle\\
&\quad-\frac{1}{N}\sum_q\Big\{V_2(C_1\cos k_x-C_2\gamma_{2k})\cos q_x\\
&\quad+V_2'\Big(-\frac{3}{8}+C_1\cos k_y-\frac{C_3}{2}\cos 2k_y\Big)\cos q_y\Big\}\left\langle b_{q\uparrow}b_{-q\downarrow}\right\rangle. \qquad (12)
\end{aligned}
$$

Here $I_k=4I\gamma_{1k}$, $\phi_k=\cos\frac{k_x}{2}\cos\frac{k_y}{2}$, $\psi_k=\sin\frac{k_x}{2}\sin\frac{k_y}{2}$, and the average

$$
\begin{aligned}
\left\langle u_{q\uparrow}u_{-q\downarrow}\right\rangle = &-s_{q,x}^2\left\langle a_{q\uparrow}a_{-q\downarrow}\right\rangle-s_{q,y}^2\left\langle b_{q\uparrow}b_{-q\downarrow}\right\rangle\\
&-\psi_q\big(\left\langle a_{q\uparrow}b_{-q\downarrow}\right\rangle+\left\langle b_{q\uparrow}a_{-q\downarrow}\right\rangle\big). \qquad (13)
\end{aligned}
$$

When deriving the system (9), we assume that the state of the localized momenta corresponds to the quantum spin liquid. In this case, the spin correlation functions $C_j = \langle \mathbf{S}_0 \mathbf{S}_{r_j} \rangle$ arising in (10) and (12) satisfy the relations

$$C_j = 3\left\langle S_0^x S_{r_j}^x \right\rangle = 3\left\langle S_0^y S_{r_j}^y \right\rangle = 3\left\langle S_0^z S_{r_j}^z \right\rangle, \tag{14}$$

where r_j is the position of a copper ion within the coordination sphere j. Besides, $\langle S_f^x \rangle = \langle S_f^y \rangle = \langle S_f^z \rangle = 0$.

In the course of deriving the fifth equation in (12), the relation

$$\begin{aligned}\left\langle \left(\mathbf{S}_f \boldsymbol{\sigma}_{\downarrow\alpha} c_{k\alpha}\right)\left(\mathbf{S}_g \boldsymbol{\sigma}_{\uparrow\beta} c_{p\beta}\right)\right\rangle &= 2\left\langle \left(\mathbf{S}_f \mathbf{S}_g\right) c_{k\uparrow} c_{p\downarrow}\right\rangle \\ &\quad - \left\langle \left(\mathbf{S}_f \boldsymbol{\sigma}_{\downarrow\alpha} c_{p\alpha}\right)\left(\mathbf{S}_g \boldsymbol{\sigma}_{\uparrow\beta} c_{k\beta}\right)\right\rangle \end{aligned} \tag{15}$$

is used for the averages with operators not reducing to the basis ones. Here, we mean summation over indices α and β. The relation (15) is justified within the SU(2)-invariant phase and allows one to express some average through an average consisting of the basis operators. The use of relation (15) for the component of the superconducting-order parameter Δ_{5k} under summation sign in (12) leads to an appearance of the anomalous average $\langle L_{q\uparrow} L_{-q,\downarrow} \rangle$ playing the key role in the implementation of the superconducting d-wave pairing in an ensemble of the spin-polaron quasiparticles. For the thermodynamic means consisting of the scalar product of spin operators, the decoupling procedure is used. As a result, the magnetic correlator C_1 appears in the first term on the right of the expression for Δ_{5k}.

Directly after calculation of the commutators, the contribution of the intersite Coulomb interaction to Δ_{5k} has the form

$$\begin{aligned}&-\frac{4V_1}{N} \sum_{\substack{1,2,3,4 \\ \alpha\beta}} \phi_{1-2} s_{1x} s_{3y} \delta_{1-2+3-4} \left[\left\langle (\mathbf{S}_{k-1} \boldsymbol{\sigma}_{\uparrow\alpha} a_{2\alpha})(\mathbf{S}_{-k-3} \boldsymbol{\sigma}_{\downarrow\beta} b_{4\beta}) \right\rangle \right. \\ &\left. + \left\langle (\mathbf{S}_{k-3} \boldsymbol{\sigma}_{\uparrow\alpha} b_{4\alpha})(\mathbf{S}_{-k-1} \boldsymbol{\sigma}_{\downarrow\beta} a_{2\beta}) \right\rangle \right], \end{aligned} \tag{16}$$

where $\mathbf{S}_k = \dfrac{1}{N} \sum_f e^{-ikf} \mathbf{S}_f$ is the Fourier transform of a spin operator. As far as the operators standing under the average cannot be reduced to the basis operators, even after the use of the relation (15), we perform the decoupling procedure to the averages (16) taking into account the SU(2)-invariance of the spin subsystem. This procedure gives rise to the term proportional to V_1 in the fifth equation (12).

Note that we neglect the contributions proportional to "density–density" correlators arising as a result of decoupling of the averages in (10) and (12), because we consider the case of low doping.

It follows from the analysis of the system (9) in the normal phase that the fermionic excitations spectrum of the quasiparticles within the SFM is determined by the solutions of the dispersion equation

$$\begin{aligned}\det{}_k(\omega) &= (\omega - \xi_x)(\omega - \xi_y)(\omega - \xi_L) - 2J_x J_y t_k K_k \\ &\quad -(\omega - \xi_y) J_x^2 K_k - (\omega - \xi_x) J_y^2 K_k - (\omega - \xi_L) t_k^2 = 0. \end{aligned} \tag{17}$$

The spectrum consists of three bands ε_{1k}, ε_{2k} and ε_{3k} [66]. The branch ε_{1k} with the minimum at a point close to $(\pi/2, \pi/2)$ of the Brillouin zone arises owing to the strong spin-fermion coupling inducing both the exchange interaction between holes and the localized spins at the nearest copper ions and spin-correlated hoppings. At the low doping, the dynamics of holes is determined by the lower band ε_{1k}.

4 Equations for the Components of the Superconducting-Order Parameter

To analyse the Cooper instability, we express the anomalous Green's functions in terms of the Δ^*_{lk} parameters in the linear approximation

$$F_{ij}(k,\omega) = \sum_{i,j=1}^{3} \sum_{l=1}^{5} \frac{S^{(l)}_{ij}(k,\omega)}{\mathrm{Det}_k(\omega)} \Delta^*_{lk}. \tag{18}$$

Actual Green's functions are $F_{11}(k,\omega)$, $F_{12}(k,\omega)$, $F_{21}(k,\omega)$, $F_{22}(k,\omega)$, $F_{31}(k,\omega)$, $F_{32}(k,\omega)$ and $F_{33}(k,\omega)$. Here, $\mathrm{Det}_k(\omega) = -\det_k(\omega)\det_k(-\omega)$, while the corresponding functions $S^{(l)}_{ij}(k,\omega)$ are listed in "Appendix".

Using the spectral theorem [67], we find the expressions for the anomalous averages and finally arrive at the closed set of uniform integral equations for the superconducting-order parameters ($l = 1, \ldots, 5$)

$$\begin{aligned}
\Delta^*_{1k} &= -\frac{2}{N} \sum_{lq} \left(\frac{U_p}{2} + V_2 \cos k_y \cos q_y + V_2' \cos k_x \cos q_x \right) M^{(l)}_{11}(q) \Delta^*_{lq}, \\
\Delta^*_{2k} &= -\frac{4V_1}{N} \sum_{lq} \phi_{k-q} M^{(l)}_{21}(q) \Delta^*_{lq}, \\
\Delta^*_{3k} &= -\frac{4V_1}{N} \sum_{lq} \phi_{k-q} M^{(l)}_{12}(q) \Delta^*_{lq}, \\
\Delta^*_{4k} &= -\frac{2}{N} \sum_{lq} \left(\frac{U_p}{2} + V_2 \cos k_x \cos q_x + V_2' \cos k_y \cos q_y \right) M^{(l)}_{22}(q) \Delta^*_{lq}, \\
\Delta^*_{5k} &= -\frac{1}{N} \sum_{lq} R^{(l)}_0(q) \Delta^*_{lq} + \frac{1}{N} \sum_{lq} I_{k-q} R^{(l)}_{1a}(q) \Delta^*_{lq} \\
&\quad + \cos k_x \frac{1}{N} \sum_{lq} R^{(l)}_{1b}(q) \Delta^*_{lq} + \cos k_y \frac{1}{N} \sum_{lq} R^{(l)}_{1c}(q) \Delta^*_{lq} \\
&\quad - \gamma_{2k} \frac{1}{N} \sum_{lq} R^{(l)}_2(q) \Delta^*_{lq} - \sin k_x \sin k_y \frac{1}{N} \sum_{lq} \phi_q R^{(l)}_3(q) \Delta^*_{lq} \\
&\quad - \cos 2k_x \frac{1}{N} \sum_{lq} R^{(l)}_{4a}(q) \Delta^*_{lq} - \cos 2k_y \frac{1}{N} \sum_{lq} R^{(l)}_{4b}(q) \Delta^*_{lq},
\end{aligned} \tag{19}$$

where the following functions are introduced:

$$
\begin{aligned}
R_0^{(l)}(q) &= \frac{3}{4}V_1\psi_q M_{ab}^{(l)}(q) + 2J\gamma_{1q}M_{33}^{(l)}(q) \\
&\quad - (8IC_1 + 3J/2)M_{uu}^{(l)}(q) + \frac{3}{8}U_p(M_{11}^{(l)}(q) + M_{22}^{(l)}(q)) \\
&\quad - 2\left(\xi(q_x)s_{q,x} + t_q s_{q,y}\right)M_{31}^{(l)}(q) - 2\left(\xi(q_y)s_{q,y} + t_q s_{q,x}\right)M_{32}^{(l)}(q) \\
&\quad - \frac{3}{8}V_2'\cos q_x M_{11}^{(l)}(q) - \frac{3}{8}V_2'\cos q_y M_{22}^{(l)}(q), \\
R_{1a}^{(l)}(q) &= M_{33}^{(l)}(q) - C_1 M_{uu}^{(l)}(q), \\
R_{1b}^{(l)}(q) &= C_1\big(V_1\psi_q M_{ab}^{(l)}(q) - 2JM_{uu}^{(l)}(q) + U_p M_{11}^{(l)}(q) \\
&\quad - V_2'\cos q_x M_{11}^{(l)}(q) - V_2\cos q_x M_{22}^{(l)}(q)\big), \\
R_{1c}^{(l)}(q) &= C_1(V_1\psi_q M_{ab}^{(l)}(q) - 2JM_{uu}^{(l)}(q) + U_p M_{22}^{(l)}(q) \\
&\quad - V_2\cos q_y M_{11}^{(l)}(q) - V_2'\cos q_y M_{22}^{(l)}(q)), \\
R_2^{(l)}(q) &= C_2\left(V_1\psi_q M_{ab}^{(l)}(q) - V_2\cos q_y M_{11}^{(l)}(q) - V_2\cos q_x M_{22}^{(l)}(q))\right), \\
R_3^{(l)}(q) &= V_1 C_2 M_{ab}^{(l)}(q), \\
R_{4a}^{(l)}(q) &= -\frac{V_2'}{2}C_3\cos q_x M_{11}^{(l)}(q), \\
R_{4b}^{(l)}(q) &= -\frac{V_2'}{2}C_3\cos q_y M_{22}^{(l)}(q), \\
M_{uu}^{(l)}(q) &= -s_{qx}^2 M_{11}^{(l)}(q) - s_{qy}^2 M_{22}^{(l)}(q) - \psi_q M_{ab}^{(l)}(q), \\
M_{ab}^{(l)}(q) &= M_{21}^{(l)}(q) + M_{12}^{(l)}(q), \\
M_{nm}^{(l)}(q) &= \frac{S_{nm}^{(l)}(q, E_{1q}) + S_{nm}^{(l)}(q, -E_{1q})}{4E_{1q}(E_{1q}^2 - E_{2q}^2)(E_{1q}^2 - E_{3q}^2)}\tanh\left(\frac{E_{1q}}{2T}\right).
\end{aligned}
\tag{20}
$$

Here E_{jq} are the branches of the Fermi excitation spectrum which can be found from the dispersion equation $\mathrm{Det}_k(\omega) = 0$ in the superconducting phase. Below, we use the system (19) to find the critical superconducting temperature of the spin-polaron quasiparticles with specified types of the order parameter symmetry.

5 Implementation of the Superconducting *d*- and *s*-Wave Pairings of Spin Polarons

One can see from the system (19) that the kernels of the integral equations are split. Therefore, we can seek a solution of (19) in the form

$$
\begin{aligned}
\Delta_{1k} &= B_{11} + B_{12}\cos k_x + B_{13}\cos k_y, \\
\Delta_{2k} &= B_{21}\phi_k + B_{22}\psi_k, \\
\Delta_{3k} &= B_{31}\phi_k + B_{32}\psi_k,
\end{aligned}
$$

$$\begin{aligned}\Delta_{4k} &= B_{41} + B_{42}\cos k_x + B_{43}\cos k_y,\\ \Delta_{5k} &= B_{51} + B_{52}\cos k_x + B_{53}\cos k_y + B_{54}\cos k_x\cos k_y\\ &\quad + B_{55}\sin k_x \sin k_y + B_{56}\cos 2k_x + B_{57}\cos 2k_y,\end{aligned} \tag{21}$$

where the seventeen amplitudes B define the contribution of the corresponding basis functions in the expansion of the order parameter components. Substituting these expressions into (19) and equating the coefficients of the corresponding trigonometric functions, we obtain the system of seventeen algebraic equations for the amplitudes B. Solving this system with regard to the equation for the chemical potential μ, we find the doping dependence of the critical temperature of the transition to the superconducting phase $T_c(x)$ for different types of the order parameter symmetry. When obtaining the equation for μ, we take into account that in the limit of $T \to T_c$ all the components of the order parameter $\Delta_{jk} \to 0$. As a result, we obtain the equation for the chemical potential

$$x = \frac{2}{N}\sum_q \frac{f(\varepsilon_{1q})\left[Q_{3x}(q,\varepsilon_{1q}) + Q_{3y}(q,\varepsilon_{1q})\right]}{\left(\varepsilon_{1q}-\varepsilon_{2q}\right)\left(\varepsilon_{1q}-\varepsilon_{3q}\right)}, \tag{22}$$

where x is the doping level, $f(E) = (e^{E/T}+1)^{-1}$ is the Fermi–Dirac distribution function and functions $Q_{3x}(k,\omega)$ and $Q_{3y}(k,\omega)$ are given in "Appendix".

The self-consistent solutions of the seventeen equations for the amplitudes B with regard to the equation for the chemical potential are presented in Fig. 2. The thin black dashed curve shows the critical temperature for the transition to the superconducting

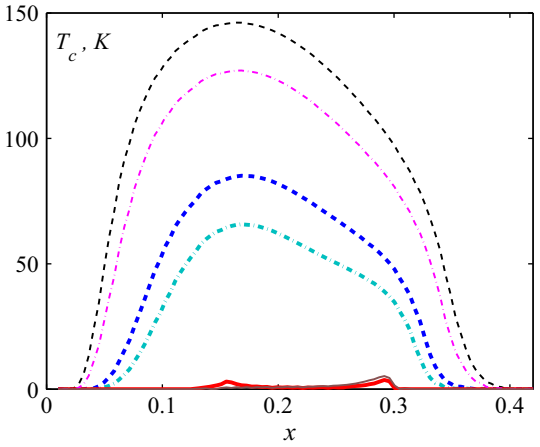

Fig. 2 Critical temperatures for the transition to the superconducting $d_{x^2-y^2}$ phase versus doping x calculated for the set of parameters $J = 3.38$, $\tau = 0.10$, $t = 0.12$, $I = 0.136$ at $U_p = V_2 = V_2' = 0$ (thin black dashed curve), $U_p = 0$, $V_2 = V_2' = 0.1$ (thin magenta dash-dotted curve), $U_p = 3$, $V_2 = V_2' = 0$ (bold blue dashed curve), $U_p = 3$, $V_2 = V_2' = 0.1$ (bold green dash-dotted curve), $U_p = 0$, $V_2 = V_2' = 0.8$ (thin brown curve) and $U_p = 3$, $V_2 = V_2' = 0.5$ (bold red curve). All the parameters are given in units of eV (Color figure online)

$d_{x^2-y^2}$ phase versus doping at $U_p = V_1 = V_2 = V_2' = 0$. An important aspect of our approach is that an accounting for the Coulomb interaction between the nearest neighbors V_1 does not affect the dependence $T_c(x)$ for the $d_{x^2-y^2}$-wave pairing, i.e., the thin black dashed curve is robust with respect to taking into account $V_1 \neq 0$ [51]. The cause of such a behavior can be revealed after analysis of the solutions (21) of the system (19). In the range of doping, where the d-wave pairing is implemented at $T \lesssim T_c$, the solutions of the algebraic system for the amplitudes B show that only four of them B_{52}, B_{53}, B_{22}, B_{32} are not equal to zero, besides, $B_{52} = -B_{53}$, $B_{22} = -B_{32}$ and $|B_{52}|/|B_{22}| \sim 10^3$. This means that the quasimomentum dependence of the superconducting gap is mainly caused by the fifth component of the order parameter Δ_{5k} which has the form

$$\Delta_{5k}^{(d)} = B_{52} \cdot (\cos k_x - \cos k_y). \tag{23}$$

For the d-wave pairing at $U_p = V_2 = V_2' = 0$ the amplitudes B_{52} and B_{53} in the equation for Δ_{5k} are defined by the exchange coupling constant I rather than by parameter V_1. Therefore, we come to the conclusion that the intersite Coulomb repulsion between holes located at the nearest oxygen sites does not suppress the superconducting $d_{x^2-y^2}$-wave pairing [51].

Thus, in the case of the d-wave pairing at $U_p = V_2 = V_2' = 0$, instead of the system of seventeen equations, we can obtain and solve a simple equation for the critical temperature T_c [66,68,69]. This equation follows from the fifth equation of the system (19) and has the form

$$1 = \frac{I}{N} \sum_q (\cos q_x - \cos q_y)^2 \left(M_{33}^{(5)}(q, \varepsilon_{1q}) - C_1 M_{uu}^{(5)}(q, \varepsilon_{1q}) \right). \tag{24}$$

In particular, it follows from (24) that the exchange interaction between the spin momenta of copper ions acts as a mechanism enhancing the Cooper instability, in a way that this interaction is transformed into an effective attraction owing to the strong spin-charge coupling. Naturally, the solution of Eq. (24) and the system of seventeen equations for the d-wave pairing is exactly the same and is shown with the thin black dashed curve in Fig. 2.

Accounting for the Coulomb repulsion U_p between two holes located on the same oxygen ion in contrast to the intersite Coulomb interaction V_1 leads to the suppression for the superconducting d-wave pairing. However, the comparison of the bold blue dashed curve ($U_p = 3\,\text{eV}$, $V_2 = V_2' = 0$) and the thin black dashed curve ($U_p = V_2 = V_2' = 0$) in Fig. 2 shows that this suppression is not crucial for the implementation of high-temperature superconductivity, because at the optimal doping level $x \simeq 0.16$ the critical temperature holds high values.

It follows from the system (19) that one should seek the solution for the superconducting s-wave pairing in the form

$$\Delta_{1k}^{(s)} = \Delta_{4k}^{(s)} = B_1,$$
$$\Delta_{2k}^{(s)} = \Delta_{3k}^{(s)} = 0,$$

$$\Delta_{5k}^{(s)} = B_3 + 2B_{cx}\gamma_{1k} + B_{cc}\gamma_{2k}. \quad (25)$$

The calculations show that in this case the system of seventeen equations for the amplitudes B has no nontrivial solutions. Consequently, within the SFM, which takes into account the exchange energy between the localized and itinerant spins rigorously, the superconducting s-wave pairing is not implemented. This is the main difference of our theory of high-temperature superconductivity from theories based on effective single-band models of strongly correlated electrons on a square lattice, in which, along with the superconducting d-wave pairing, there always exists a solution for the s-wave pairing.

Let us consider the influence of the intersite Coulomb repulsion V_2 and V_2' between holes located at the next-nearest-neighbor oxygen ions of the CuO_2 plane on superconducting pairing. In Fig. 2, the thin magenta dash-dotted line depicts the dependence $T_c(x)$ obtained for $U_p = 0,\ V_2 = V_2' = 0.1$ eV and the thin brown curve corresponds to $T_c(x)$ for $U_p = 0,\ V_2 = V_2' = 0.8$ eV. One can see that the inclusion of V_2 and V_2', in contrast to the interaction V_1, leads to the suppression of the $d_{x^2-y^2}$-wave pairing. Besides, this suppression becomes stronger if $U_p \neq 0$ (the bold green dash-dotted and the bold red curves). However, the superconducting $d_{x^2-y^2}$-wave pairing appears to be robust toward the influence of the intersite Coulomb repulsion between holes located at the next-nearest-neighbor oxygen ions of the CuO_2 plane and can be suppressed only at unrealistic large values $V_2,\ V_2' > 0.5$ eV.

6 Conclusion

In conclusion, we have shown that the neutralization of the negative influence of the intersite Coulomb interaction in the superconducting d-wave channel of cuprate superconductors is caused by two factors. The main factor is connected with the consideration of the real crystalline structure of the CuO_2 plane. In accordance with this factor, the Coulomb repulsion between fermions in the oxygen sublattice is described by the corresponding Fourier transform

$$V_q = 4V_1 \cos(q_x/2)\cos(q_y/2).$$

The second factor is caused by strong electron correlations. These correlations lead to the appearance of the strong coupling between the localized copper spins and the oxygen holes. As a result, the formation of spin-polaron quasiparticles occurs in the system, and the Cooper instability appears between these quasiparticles. In this case, the Coulomb repulsion between bare holes with the Fourier transform V_q is renormalized into the interaction between the spin-polaron quasiparticles in such a way that the quasimomentum dependence of this effective interaction corresponds to the structure of the copper ions sublattice. As a result, it occurs that the effective repulsion between spin polarons vanishes in the equation for the superconducting d-wave pairing. At the same time, for the Cooper instability in the s-wave channel, the contribution of the noted effective repulsion remains.

Despite this fact, our self-consistent calculations show that within the spin-fermion model only the superconducting d-wave pairing is implemented, whereas solutions for the s-wave pairing are absent for all admissible doping levels. These results agree with the experimental data on cuprate superconductors. In this connection, it should be noted that in the framework of the $t-J$ model in the region of doping levels relevant for the cuprates, the superconducting s-wave pairing is implemented and the corresponding critical temperatures significantly exceed T_c for the d-wave pairing. Concerning the differences that arose, it is appropriate to point out that within our approach the copper spins subsystem plays an essential role. This subsystem is separated from that of holes at oxygen ions, whereas within the $t-J$ model, the electron and spin degrees of freedom refer to the same fermions.

Finally, we have shown that the intersite Coulomb repulsion between holes located at the next-nearest-neighbor oxygen ions of the CuO_2 plane suppresses the $d_{x^2-y^2}$-wave pairing only at unphysically large values of these interactions. Taking into account our previous result [51] on neutralization for the effect of the Coulomb interaction V_1 for the nearest-neighbor oxygen sites, we conclude that accounting for the real structure of the CuO_2 plane leads to stability of the $d_{x^2-y^2}$-wave pairing toward the strong intersite Coulomb repulsion. It is obvious that taking into account the Coulomb interaction V_3 does not affect the superconducting d-wave pairing because of the same symmetry reason as that for V_1 [51].

Note that the difference in the contributions of the Coulomb interaction to the implementation of different superconducting phases also manifests itself in the Kohn–Luttinger theory of superconductivity [70]. In this theory, the long-range Coulomb repulsions within the lattice models usually contribute only to certain pairing channels and do not affect the other channels. At the same time, the polarization contributions have components in all the channels, and more than one of them usually plays in favor of attraction. As a result, according to the authors [20–22], the intersite Coulomb repulsion either does not affect at all the main component of the effective interaction leading to pairing, or it suppresses the principal component without influencing the secondary ones. However, in our case, the key role is played by the spatial separation between two types of oxygen orbitals.

Acknowledgements The work was supported by the program of the Presidium of the Russian Academy of Sciences No. 12 "Fundamental problems of high-temperature superconductivity", the Russian Foundation for Basic Research (RFBR) and partly by the Government of Krasnoyarsk Region and the Krasnoyarsk Region Science and Technology Support Fund (Projects Nos. 16-42-243057 and 16-42-240435). The work of A. F. B. was funded by RFBR (Project No. 16-02-00304). The work of M. M. K. was supported by a grant of the President of the Russian Federation (Project MK-1398.2017.2).

Appendix

The functions $S_{ij}^{(l)}(k,\omega)$ in anomalous Green's functions $F_{ij}(k,\omega)$ have the form

$$S_{11}^{(1)}(k,\omega) = Q_{3y}(k,-\omega)Q_{3y}(k,\omega),$$
$$S_{11}^{(2)}(k,\omega) = S_{21}^{(1)}(k,\omega) = Q_{3}(k,-\omega)Q_{3y}(k,\omega),$$

$$
\begin{aligned}
&S_{11}^{(3)}(k,\omega) = S_{12}^{(1)}(k,\omega) = S_{11}^{(2)}(k,-\omega),\\
&S_{11}^{(4)}(k,\omega) = S_{12}^{(2)}(k,\omega) = S_{21}^{(3)}(k,\omega) = S_{22}^{(1)}(k,\omega) = Q_3(k,-\omega)Q_3(k,\omega),\\
&S_{11}^{(5)}(k,\omega) = -Q_y(k,-\omega)Q_y(k,\omega),\\
&S_{12}^{(3)}(k,\omega) = Q_{3y}(k,-\omega)Q_{3x}(k,\omega),\\
&S_{21}^{(2)}(k,\omega) = S_{12}^{(3)}(k,-\omega),\\
&S_{12}^{(4)}(k,\omega) = S_{22}^{(3)}(k,\omega) = Q_3(k,-\omega)Q_{3x}(k,\omega),\\
&S_{21}^{(4)}(k,\omega) = S_{22}^{(2)}(k,\omega) = S_{12}^{(4)}(k,-\omega),\\
&S_{12}^{(5)}(k,\omega) = -Q_y(k,-\omega)Q_x(k,\omega),\\
&S_{21}^{(5)}(k,\omega) = S_{12}^{(5)}(k,-\omega),\\
&S_{22}^{(4)}(k,\omega) = Q_{3x}(k,-\omega)Q_{3x}(k,\omega),\\
&S_{22}^{(5)}(k,\omega) = -Q_x(k,-\omega)Q_x(k,\omega),\\
&S_{31}^{(1)}(k,\omega) = -K_k Q_y(k,-\omega)Q_{3y}(k,\omega),\\
&S_{31}^{(2)}(k,\omega) = -K_k Q_x(k,-\omega)Q_{3y}(k,\omega),\\
&S_{31}^{(3)}(k,\omega) = S_{32}^{(1)}(k,\omega) = -K_k Q_y(k,-\omega)Q_3(k,\omega),\\
&S_{31}^{(4)}(k,\omega) = S_{32}^{(2)}(k,\omega) = -K_k Q_x(k,-\omega)Q_3(k,\omega),\\
&S_{31}^{(5)}(k,\omega) = Q_{xy}(k,-\omega)Q_y(k,\omega),\\
&S_{32}^{(3)}(k,\omega) = -K_k Q_y(k,-\omega)Q_{3x}(k,\omega),\\
&S_{32}^{(4)}(k,\omega) = -K_k Q_x(k,-\omega)Q_{3x}(k,\omega),\\
&S_{32}^{(5)}(k,\omega) = Q_{xy}(k,-\omega)Q_x(k,\omega),\\
&S_{33}^{(1)}(k,\omega) = -K_k^2 S_{11}^{(5)}(k,\omega),\\
&S_{33}^{(2)}(k,\omega) = K_k^2 S_{12}^{(5)}(k,-\omega),\\
&S_{33}^{(3)}(k,\omega) = S_{33}^{(2)}(k,-\omega),\\
&S_{33}^{(4)}(k,\omega) = K_k^2 S_{22}^{(5)}(k,\omega),\\
&S_{33}^{(5)}(k,\omega) = Q_{xy}(k,-\omega)Q_{xy}(k,\omega).
\end{aligned}
\tag{26}
$$

where

$$
\begin{aligned}
&Q_{x(y)}(k,\omega) = (\omega-\xi_{x(y)})J_{y(x)} + t_k J_{x(y)}, \qquad Q_{xy}(k,\omega) = (\omega-\xi_x)(\omega-\xi_y) - t_k^2,\\
&Q_{3x(3y)}(k,\omega) = (\omega-\xi_L)(\omega-\xi_{x(y)}) - J_{x(y)}^2 K_k, \quad Q_3(k,\omega) = (\omega-\xi_L)t_k + J_x J_y K_k.
\end{aligned}
$$

References

1. P.W. Anderson, Science **235**, 1196 (1987)
2. N.F. Mott, *Metal-Insulator Transitions* (Taylor & Francis, London, New York, Philadelphia, 1990)
3. J.C. Hubbard, Proc. R. Soc. Lond. A **276**, 238 (1963)

4. M. Imada, A. Fujimori, Y. Tokura, Rev. Mod. Phys. **70**, 1039 (1998)
5. E. Dagotto, Rev. Mod. Phys. **66**, 763 (1994)
6. A. Damascelli, Z. Hussain, Z.-X. Shen, Rev. Mod. Phys. **75**, 473 (2003)
7. D.J. Scalapino, E. Loh Jr., J.E. Hirsch, Phys. Rev. B **34**, 8190 (1986)
8. D.J. Scalapino, E. Loh Jr., J.E. Hirsch, Phys. Rev. B **35**, 6694 (1987)
9. R.O. Zaitsev, V.A. Ivanov, Sov. Phys. Solid State **29**, 1475 (1987)
10. H. Fukuyama, Y. Hasegawa, O. Narikiyo, J. Phys. Soc. Jpn. **60**, 2013 (1991)
11. M.A. Baranov, M.Y. Kagan, Z. Phys. B **86**, 237 (1992)
12. Y.A. Izyumov, Phys. Usp. **38**, 385 (1995)
13. D. Zanchi, H.J. Schulz, Phys. Rev. B **54**, 9509 (1996)
14. H. Tasaki, J. Phys.: Condens. Matter **68**, 4353 (1998)
15. R. Hlubina, Phys. Rev. B **59**, 9600 (1999)
16. S. Raghu, S.A. Kivelson, D.J. Scalapino, Phys. Rev. B **81**, 224505 (2010)
17. A.S. Alexandrov, V.V. Kabanov, Phys. Rev. Lett. **106**, 136403 (2011)
18. S. Shubin, S. Vonsowsky, Proc. R. Soc. A **145**, 159 (1934)
19. M.Y. Kagan, D.V. Efremov, M.S. Marienko, V.V. Val'kov, JETP Lett. **93**, 720 (2011)
20. S. Raghu, E. Berg, A.V. Chubukov, S.A. Kivelson, Phys. Rev. B **85**, 024516 (2012)
21. M.Y. Kagan, V.V. Val'kov, V.A. Mitskan, M.M. Korovushkin, JETP Lett. **97**, 226 (2013)
22. M.Y. Kagan, V.V. Val'kov, V.A. Mitskan, M.M. Korovushkin, JETP **117**, 728 (2013)
23. V.J. Emery, Phys. Rev. Lett. **58**, 2794 (1987)
24. F.C. Zhang, T.M. Rice, Phys. Rev. B **37**, 3759 (1988)
25. J.H. Jefferson, H. Eskes, L.F. Feiner, Phys. Rev. B **45**, 7959 (1992)
26. V.I. Belinicher, A.L. Chernyshev, Phys. Rev. B **47**, 390 (1993)
27. L.F. Feiner, J.H. Jefferson, R. Raimondi, Phys. Rev. B **53**, 8751 (1996)
28. V. Gavrichkov, A. Borisov, S.G. Ovchinnikov, Phys. Rev. B **64**, 235124 (2001)
29. D.J. Scalapino, Phys. Rep. **250**, 329 (1995)
30. Y.A. Izyumov, Phys. Usp. **40**, 445 (1997)
31. Y.A. Izyumov, Phys. Usp. **42**, 215 (1999)
32. T. Moriya, K. Ueda, Rep. Prog. Phys. **66**, 1299 (2003)
33. N.M. Plakida, *High-Temperature Cuprate Superconductors* (Springer, Berlin, 2010)
34. R.O. Zaitsev, JETP **98**, 780 (2004)
35. V.V. Val'kov, M.M. Korovushkin, JETP **112**, 108 (2011)
36. V.Y. Yushankhai, G.M. Vujicic, R.B. Zakula, Phys. Lett. A **151**, 254 (1990)
37. V.V. Val'kov, T.A. Val'kova, D.M. Dzebisashvili, S.G. Ovchinnikov, JETP Lett. **75**, 378 (2002)
38. N.M. Plakida, V.S. Oudovenko, Eur. Phys. J. B **86**, 115 (2013)
39. N.M. Plakida, V.S. Oudovenko, JETP **146**, 631 (2014)
40. E.I. Shneyder, S.G. Ovchinnikov, JETP **109**, 1017 (2009)
41. T. Misawa, M. Imada, Phys. Rev. B **90**, 115137 (2014)
42. N.M. Plakida, Phys. C **531**, 39 (2016)
43. V.A. Gavrichkov, S.G. Ovchinnikov, A.A. Borisov, E.G. Goryachev, JETP **91**, 369 (2000)
44. V.V. Val'kov, D.M. Dzebisashvili, A.F. Barabanov, Theor. Math. Phys. **191**, 752 (2017)
45. V.V. Val'kov, V.A. Mitskan, D.M. Dzebisashvili, A.F. Barabanov, Low Temp. Phys. **44**, 173 (2018)
46. H. Matsukawa, H. Fukuyama, J. Phys. Soc. Jpn. **58**, 2845 (1989)
47. C.M. Varma, S. Schmitt-Rink, E. Abrahams, Solid State Commun. **62**, 681 (1987)
48. P. Monthoux, D. Pines, G.G. Lonzarich, Nature **450**, 1177 (2007)
49. H. Fröhlich, Phys. Rev. **79**, 845 (1950)
50. V.V. Tolmachev, Dokl. Akad. Nauk SSSR **140**, 563 (1961). [in Russian]
51. V.V. Val'kov, D.M. Dzebisashvili, M.M. Korovushkin, A.F. Barabanov, JETP Lett. **103**, 385 (2016)
52. A.F. Barabanov, L.A. Maksimov, G.V. Uimin, JETP Lett. **47**, 622 (1988)
53. A.F. Barabanov, L.A. Maksimov, G.V. Uimin, Sov. Phys. JETP **69**, 371 (1989)
54. P. Prelovšek, Phys. Lett. A. **126**, 287 (1988)
55. J. Zaanen, A.M. Oleś, Phys. Rev. B. **37**, 9423 (1988)
56. E.B. Stechel, D.R. Jennison, Phys. Rev. B. **38**, 4632 (1988)
57. V.J. Emery, G. Reiter, Phys. Rev. B. **38**, 4547 (1988)
58. M.S. Hybertsen, M. Schluter, N.E. Christensen, Phys. Rev. B **39**, 9028 (1989)
59. M. Ogata, H. Fukuyama, Rep. Prog. Phys. **71**, 036501 (2008)
60. D.M. Dzebisashvili, V.V. Val'kov, A.F. Barabanov, JETP Lett. **98**, 528 (2013)

61. M.H. Fischer, E.-A. Kim, Phys. Rev. B **84**, 144502 (2011)
62. R. Zwanzig, Phys. Rev. **124**, 983 (1961)
63. H. Mori, Prog. Theor. Phys. **33**, 423 (1965)
64. A.F. Barabanov, A.A. Kovalev, O.V. Urazaev, A.M. Belemuk, R. Hayn, JETP **92**, 677 (2001)
65. V.V. Val'kov, D.M. Dzebisashvili, A.F. Barabanov, JETP **118**, 959 (2014)
66. V.V. Val'kov, D.M. Dzebisashvili, A.F. Barabanov, Phys. Lett. A **379**, 421 (2015)
67. D.N. Zubarev, Sov. Phys. Usp. **3**, 320 (1960)
68. V.V. Val'kov, D.M. Dzebisashvili, A.F. Barabanov, J. Low Temp. Phys. **181**, 134 (2015)
69. V.V. Val'kov, D.M. Dzebisashvili, A.F. Barabanov, J. Supercond. Nov. Magn. **29**, 1049 (2016)
70. M.Y. Kagan, V.A. Mitskan, M.M. Korovushkin, Phys. Usp. **58**, 733 (2015)